Deep–Sea Research I 117 (2016) 84–94

Contents lists available at ScienceDirect

Deep–Sea Research I

journal homepage: www.elsevier.com/locate/dsri

Climate relevant trace gases (N_2O and CH_4) in the Eurasian Basin (Arctic Ocean)

Josefa Verdugo[a], Ellen Damm[b], Pauline Snoeijs[c], Beatriz Díez[d], Laura Farías[e,*]

[a] Graduate Program in Oceanography, Department of Oceanography, University of Concepcion, Concepcion, Chile
[b] Alfred-Wegener-Institute Helmholtz-Centre for Polar and Marine Reasearch, Bremerhaven, Germany
[c] Department of Ecology, Environment and Plant Sciences, Stockholm University, Svante Arrhenius väg 21A SE-10691, STOCKHOLM, Sweden
[d] Department of Molecular Genetics and Microbiology. Pontifical Catholic University of Chile and Center for Climate Change and Resilience Research (CR)^2, Santiago, Chile
[e] Laboratory of Oceanographic and Climate Processes (PROFC), Department of Oceanography, University of Concepcion and Center for Climate Change and Resilience Research (CR)^2, Concepcion, Chile

ARTICLE INFO

Keywords:
Arctic Ocean
Spatial distribution of nitrous oxide
Methane and $DMSP_t$

ABSTRACT

The concentration of greenhouse gases, including nitrous oxide (N_2O), methane (CH_4), and compounds such as total dimethylsulfoniopropionate ($DMSP_t$), along with other oceanographic variables were measured in the ice-covered Arctic Ocean within the Eurasian Basin (EAB). The EAB is affected by the perennial ice-pack and has seasonal microalgal blooms, which in turn may stimulate microbes involved in trace gas cycling. Data collection was carried out on board the LOMROG III cruise during the boreal summer of 2012. Water samples were collected from the surface to the bottom layer (reaching 4300 m depth) along a South-North transect (SNT), from 82.19°N, 8.75°E to 89.26°N, 58.84°W, crossing the EAB through the Nansen and Amundsen Basins. The Polar Mixed Layer and halocline waters along the SNT showed a heterogeneous distribution of N_2O, CH_4 and $DMSP_t$, fluctuating between 42-111 and 27–649% saturation for N_2O and CH_4, respectively; and from 3.5 to 58.9 nmol L^{-1} for $DMSP_t$. Spatial patterns revealed that while CH_4 and $DMSP_t$ peaked in the Nansen Basin, N_2O was higher in the Amundsen Basin. In the Atlantic Intermediate Water and Arctic Deep Water N_2O and CH_4 distributions were also heterogeneous with saturations between 52% and 106% and 28% and 340%, respectively. Remarkably, the Amundsen Basin contained less CH_4 than the Nansen Basin and while both basins were mostly under-saturated in N_2O. We propose that part of the CH_4 and N_2O may be microbiologically consumed via methanotrophy, denitrification, or even diazotrophy, as intermediate and deep waters move throughout EAB associated with the overturning water mass circulation. This study contributes to baseline information on gas distribution in a region that is increasingly subject to rapid environmental changes, and that has an important role on global ocean circulation and climate regulation.

1. Introduction

The extent of Arctic Ocean sea ice cover has declined since 1970, with the largest decrease reported during boreal summer months, particularly in September (Serreze et al., 2007; Serreze and Stroeve, 2015). Increased summer melting has been found to amplify biological production due to the shift from an ice-covered area to an open water surface (Arrigo et al., 2008). Ice melt also impacts microbial activity, having a profound effect on brine and the chemistry of surrounding waters, including gaseous compounds (Gleitz et al., 1995). The Arctic Ocean has significantly different oceanographic features from those in the adjacent North Atlantic and Pacific Oceans. The water masses in the Arctic Ocean have specific physical and biological signals due to the interaction of freezing and melting processes in the water column, river run-off onto the continental shelves surrounding the Arctic Basin, and advection into the Arctic Ocean (Rudels et al., 1996). In the surface layer, the most prominent feature is the presence of perennial sea ice, which varies seasonally in thickness and coverage, changing from 6×10^6 km^2 in the summer to 15×10^6 km^2 in the winter (Comiso, 2010). The sea ice cap seasonally modifies surface temperature and salinity according to sea ice freezing and melting cycles (Rudels et al., 1991). The sea ice pack also reduces light penetration and gas exchange between the surface ocean and the atmosphere, and inhibits the ventilation and mixing effect of wind on surface waters. All these processes are crucial when analyzing the gas content of surface waters, such as nitrous oxide (N_2O) and methane (CH_4). These biogenic trace

* Corresponding author.
E-mail address: laura.farias@udec.cl (L. Farías).

http://dx.doi.org/10.1016/j.dsr.2016.08.016
Received 30 September 2015; Received in revised form 30 August 2016; Accepted 30 August 2016
Available online 11 October 2016

gases contribute about 6.2% and 16% to the global greenhouse effect, respectively, also on a per molecule basis they are approximately 300 and 25 times more effective, respectively, at trapping heat than carbon dioxide (CO_2) (IPCC, 2014). N_2O also contributes to the depletion of the stratospheric ozone through photochemical reactions (Crutzen, 1991). The dissolved gas contents depend on physical and microbiological processes. During the autumn-winter period of sea ice formation, gases are expelled from the sea ice and transported to the deeper layer or vented to the atmosphere; during spring-summer, melting ice dilutes the gas content of seawater, and may produce under-saturated conditions in the surrounding waters (Anderson et al., 2004; Kitidis et al., 2010). Therefore, surface water can behave as a source or a sink of gases. Although the exact magnitude of this role is not yet fully understood, experimental efforts have been made to understand the gas transport between sea ice and sea waters in the Arctic Ocean (Loose et al., 2009).

N_2O and CH_4 play an important role in the nitrogen (N) and carbon (C) biogeochemical cycles, involved in autotrophic and heterotrophic processes (e.g., nitrification, denitrification, diazotrophy, methanotrophy and methanogenesis), which lead to their production and consumption. N_2O is mainly produced by nitrification through aerobic NH_4^+ oxidation to NO_3^- or nitrifier denitrification, the pathway through which NH_4^+ is oxidized to NO_2^- following its reduction to N_2O under oxic and also microaerophilic conditions (Wrage et al., 2001). Conversely, partial denitrification via the anaerobic reduction of NO_2^- to N_2O can produce N_2O under suboxic conditions (Codispoti and Christensen, 1985; Elkins et al., 1978) whereas the complete reduction of N-oxide to N_2 (total denitrification) is the only reaction able to consume N_2O (Elkins et al., 1978) under suboxic/anoxic conditions. The assimilative reduction of N_2O to NH_4^+, or N_2O fixation, may be responsible for a certain amount of consumption, as observed in the subtropical and cold upwelled waters of the Eastern South Pacific (Farías et al., 2013; Cornejo et al., 2015). Assimilative N_2O reduction to particulate organic nitrogen (PON) can be carried out by diazotrophic organisms through the activity of their nitrogenase enzyme, since *nif*H genes (which encodes the iron protein of the nitrogenase enzyme complex essential for biological N_2 fixation, Herrero et al., 2001; Latysheva et al., 2012; Foster et al., 2009) have been reported in Arctic sea ice and sea water (Díez et al., 2012).

CH_4 is predominantly produced or consumed biologically via methanogenesis (anaerobic organic matter respiration) and methanotrophy (aerobic methane oxidation), respectively (Reeburgh, 2007). Local methanogenesis in oxygenated waters has been suggested, known as the "methane paradox" (Lamontagne et al., 1973). Karl and Tilbrook (1994) found that methanogens living in association with zooplankton and fish fecal pellets, as well as other particulate matter, may resolve this paradox. More recently, CH_4 formation was reported to proceed the metabolism of organic methyl-compounds of methylotrophs, such as methylphosphonate (MPn) (Karl et al., 2008), dimethylsulfoniopropionate (DMSP) (Damm et al., 2010), and dimethylsulphide (DMS) (Florez-Leiva et al., 2013). Other geological/thermogenic production processes, such as CH_4 hydrates in continental margin sediments, mud volcanoes, and cold seeps, could also be responsible for CH_4 release, as is the case in the Arctic Ocean, which has been the focus of scientific interest in previous decades (Westbrook et al., 2009; Shakhova et al., 2010; Smith et al., 2014).

This research presents the spatial distribution of N_2O, CH_4 and total dimethylsulfoniopropionate ($DMSP_t$) along with other oceanographic variables collected along a South-North transect (SNT) during the LOMROG III cruise in the ice-covered Arctic Ocean, down to 4300 m depth. This study provides an essential baseline for future research in marine Polar Regions.

2. Materials and methods

Sampling was conducted in the ice-covered Arctic Ocean (Fig. 1) during the summer period (August-September 2012), onboard the Swedish Icebreaker *Oden*, along the Eurasian Basin. The transect was sampled from 82.19°N, 8.75°E to 89.26°N, 58.84°W crossing the deepest waters of the Arctic Ocean (ST 12, 11, 1, 10, 9, 8, 2, 3, 4, 5). The transect was performed across the Nansen-Gakkel Ridge from the Nansen Basin to the Amundsen Basin, between the surface (10 m) and 4300 m depth. All sample stations (except ST 12) were covered with sea ice. Hydrographic variables (temperature and salinity) were determined at sampling stations using a SBE911 plus CTD-rosette system. Water samples between 10 and 4300 m depth, including 8–16 intermediate depths, were collected with a CTD-rosette sampler equipped with 24 Niskin Bottles. Sampling for gases was carried out directly from 12 L Niskin bottles. Water samples for CH_4 (triplicate) and N_2O (triplicate) analyses were taken in 20 mL glass vials and poisoned with $HgCl_2$ (50 µL of saturated $HgCl_2$). Subsequently, the vials were sealed with a butyl-rubber septum and an aluminum cap, to avoid the formation of bubbles, and stored in darkness at room temperature until laboratory analysis. N_2O and CH_4 concentrations were analyzed by creating 5 mL of ultra-pure Helium headspace, followed by equilibration in the vial, and then quantified with a gas chromatograph. In the case of N_2O, a Shimadzu 17 A GC was used with an electron capture detector (ECD) maintained at 350 °C, and a capillary column operated at 60 °C. CH_4 was measured in a Varian 3380 GC, with flame ionization detector (FID), at 250 °C through a capillary column GS-Q in an oven at 30 °C. These instruments were connected to an autosampler device (Farías et al., 2009). A calibration curve was made with three standard concentrations for N_2O (0.1, 0.5 and 1 ppm, by Scotty Standards) and dry air, and with three standard concentrations for CH_4 (1, 5 and 10 ppm, by Scotty Standards) and dry air. Both detectors linearly responded to these concentration ranges and the analytical error for the N_2O and CH_4 measurements for this study was about 3% and 5%, respectively. Uncertainty from the measurements was calculated using the standard deviation of the triplicate measurements by depth. Samples with a variation coefficient above 10% were not taken into account for the gas database. Nutrient measurements (NO_3^-, NO_2^- and PO_4^{3-}) were performed in an automatic SEAL AA3 Autoanalyser (analytical error lower than 3%). $DMSP_t$ was measured only in the first 100 m depth. The samples were directly collected from Niskin bottles as unfiltered seawater samples, then preserved with ultrapure H_2SO_4 and stored in darkness in 50 mL polycarbonate bottles until their return to the laboratory (AWI-Germany) for further analysis. DMSP sub-samples (3 mL) were pipetted into 14 mL glass serum vials, treated with 1 mL of 5N NaOH and quickly sealed with Teflon-faced butyl rubber septa. Subsequent to alkaline cleavage, DMSP subsamples were analyzed as DMS (Kiene and Slezak, 2006). The released DMS was purged into a cryo trap and quantified with a gas chromatograph (Varian 450) equipped with a Chromosil 330 column and a pulsed flame photometric detector (PFPD) The oven temperature was 100 °C and helium was used as the purge and carrier gas.

3. Results

The distributions of oceanographic variables, including gases, were analyzed taking into consideration known water mass distribution and spatial physical gradients from Svalbard Island to Lomonosov Ridge. The SNT crossed the Nansen-Gakkel Ridge which separates the Nansen and the Amundsen Basins (Fig. 1). Profiles of oceanographic variables were grouped into three depth ranges, according water mass distribution; 1.- between the surface and 100 m depth (Polar Mixed Layer and halocline), with strong physical and biological gradients; 2.- from 100 to 900 m depth (Atlantic Intermediate Water); and 3.- from 900 to 4300 m depth (Arctic Deep Water). θS curves (Fig. 2) and vertical profiles of potential temperature and salinity (Fig. 3) support the described layering.

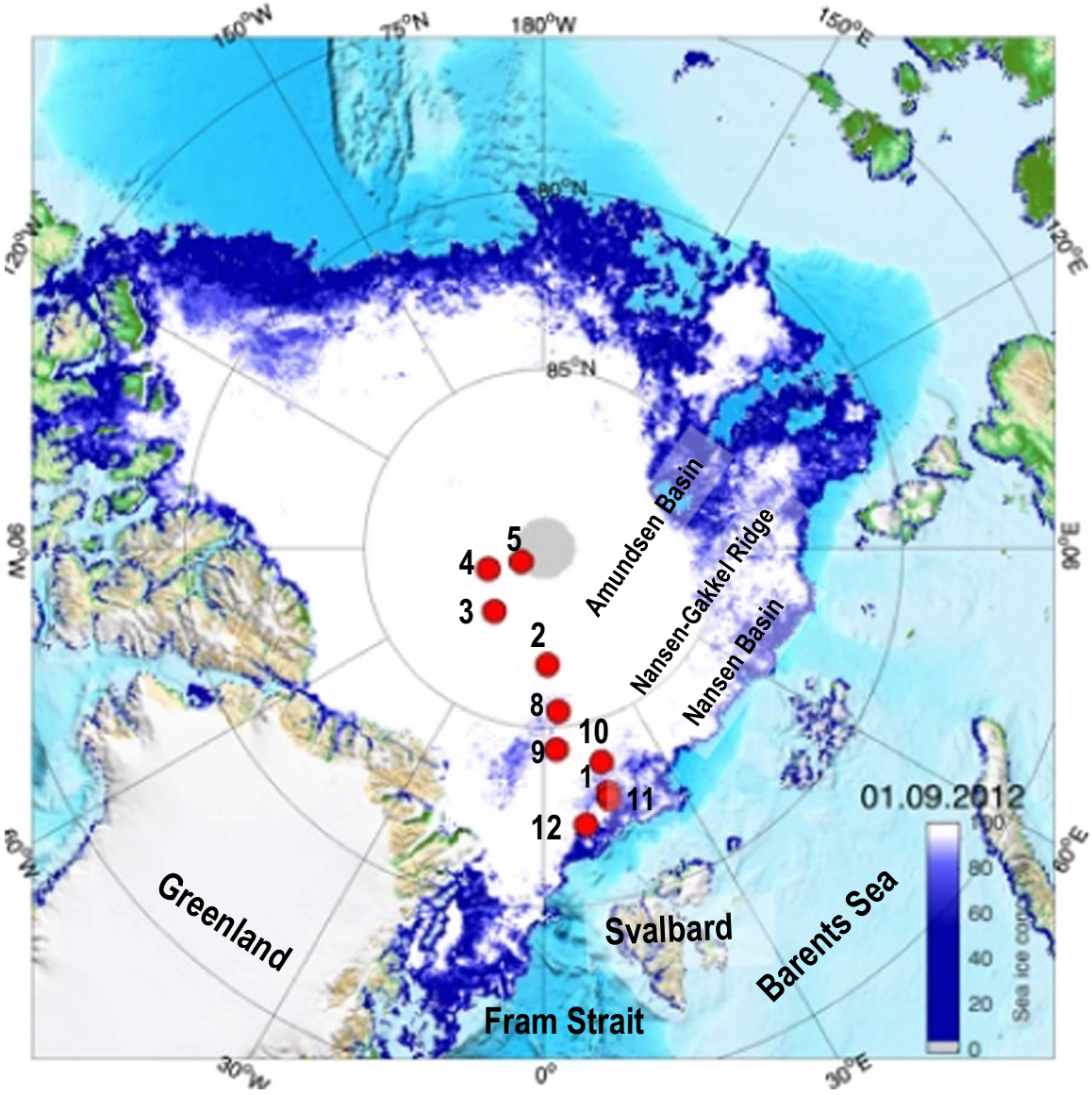

Fig. 1. Map of the Arctic Ocean during the boreal summer of 2012, with ice coverage (AMSR-E data see Spreen et al., 2008). Ice coverage is shown by colours from white to blue, (100%, 0%) meaning a closed ice cover and open water, respectively. Red dots indicate biogeochemical stations along the South-North transect; ST 12, 11, 1, 10, 9, 8, 2, 3, 4 and 5. ST 11 and 1 overlap each other. Both basins (Amundsen and Nansen) are shown on the map.

3.1. Physical variable distribution according to water mass distribution

Fig. 2 shows the θS diagram of the Polar Mixed Layer (PML) and halocline. The PML dominates the uppermost layer of the water column, between 0 and 30 m depth, and the halocline at 30–100 m depth. Potential temperature ranged from −1.8 to 0 °C, near freezing point; whereas salinity and potential density varied widely from 30.8 to 35.1 and 25.0 to 28.0 kg m^{-3}, respectively. The lowest values were found within the PML and then increased with depth. ST 12 (the station with no ice cover) presented differences with respect to the other sampled stations, with the highest temperature (3.5 °C) and salinity (35.1) values recorded along the transect, and with the greatest influence from Atlantic derived waters (Adw).

Vertical profiles of these variables along the SNT are shown in Fig. 3a. A highly stratified water column between the surface and 100 m depth was observed, a condition that hinders mixing and slows the exchange of nutrients and gases between the surface and the Atlantic Intermediate Water (AIW). In addition, differences between the Nansen and Amundsen Basins were found in terms of potential temperature and salinity, as seen in Fig. 3a. The stations closer to the south (Nansen Basin) were saltier and warmer, in contrast with the northern stations (Amundsen Basin), with fresher and colder waters.

In the AIW (100–900 m), the potential temperature and salinity varied widely from zero to 3.5 °C and 34.2 to 35.1, respectively. In this part of the water column, a warm (up to 3.5 °C), highly-saline (35.1) and dense (27.6–28.0 kg m^{-3}) water mass was found (Fig. 2). This feature is shown in Fig. 3b. This reveals that AIW enters the Arctic Ocean through the Barents Sea and the Fram Strait, the only passage which allows deep water exchange (Jones et al., 1995). Contrary, ADW (900–4300 m) is characterized by a homogenous layer with densities between 32.7 and 32.8 kg m^{-3} (Fig. 2). Potential temperature and salinity profiles (Fig. 3c) showed temperatures between −0.7 and −0.2 °C, and salinities between 34.8 and 34.9.

3.2. Biogeochemical variables according to water mass distribution

Fig. 4 illustrates the vertical cross section of nutrients and gases, and includes $DMSP_t$ at the PML and the halocline. Distributions of NO_3^- and PO_4^{3-} along the SNT were similar in both basins. NO_3^- and

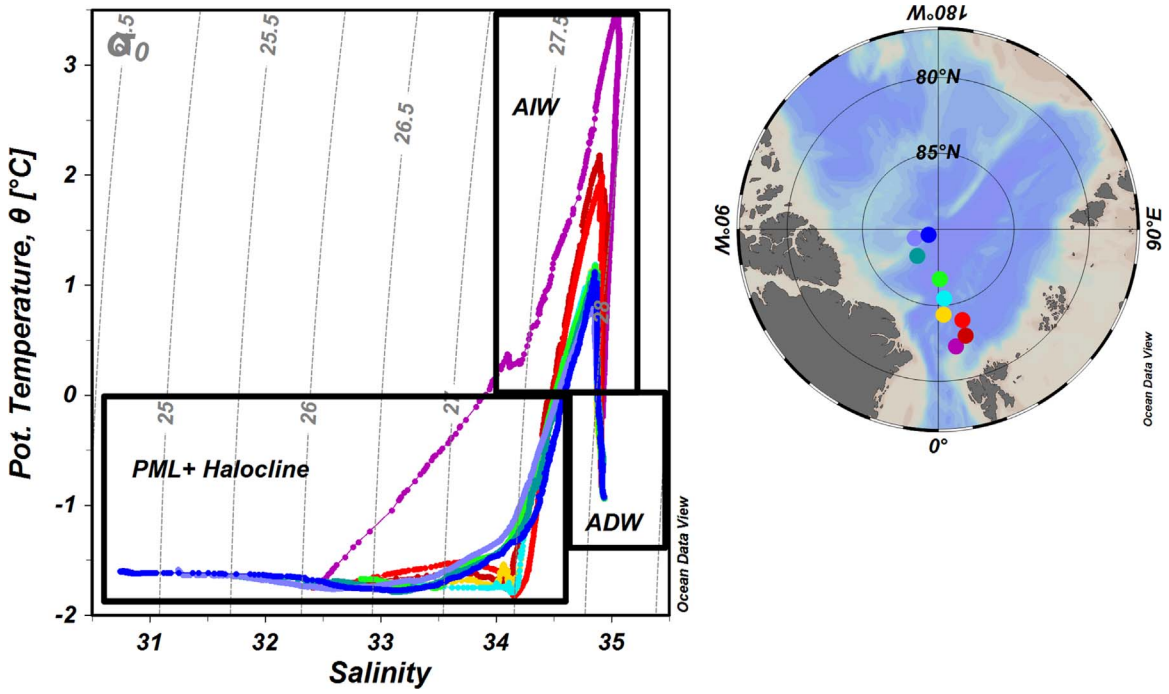

Fig. 2. θS curves from surface to 4300 m depth in the Eurasian Basin taken by Lomrog III cruise in 2012. Water mass are shown in T-S plot. PML: Polar Mixed Layer; AIW: Atlantic Intermediate Water; ADW: Arctic Deep Water.

PO_4^{3-} varied from non-detectable concentrations to 16.8 μmol L^{-1} and from 0.4 to 2.0 μmol L^{-1}, respectively (Fig. 4a; c), showing depletion between the surface and 50 m depth; except at ST 2 and ST 8 (within the Amundsen Basin), where slightly higher levels of NO_3^- (~5.0 μmol L^{-1}, at 10 m depth) were observed. PO_4^{3-} distribution was slightly depleted in surface waters, but never completely exhausted, revealing an excess of PO_4^{3-} with respect to NO_3^-, according to the Redfield ratio of 16/1. NO_3^- and PO_4^{3-} concentrations increased in the halocline reaching a maximum concentration around 16.8 and 2.0 μmol L^{-1} at 100 m depth, respectively. NO_2^- concentration (Fig. 4b) varied from zero to 0.4 μmol L^{-1} and showed an increase between 10 and 60 m depth towards the southern end of the transect (ST 11 and ST 12 within Nansen Basin). At the surface, the N/P ratio remained similar in both basins (Fig. 4d), where values as low as < 2.5 were observed between 0 and 40 m depth, and then increased with depth. However, the expected Redfield ratio (16/1) was never reached, supporting the previously mentioned P-excess. In addition, concentrations of $DMSP_t$ (Fig. 4e) varied from 3.5 to 58.9 nmol L^{-1}, peaking in the upper layer of the southward transect (Nansen Basin), showing a peak at ST 1 with the highest value around 58.9 nmol L^{-1} at 10 m depth. $DMSP_t$ concentration does not exceed 20.0 nmol L^{-1} in the Amundsen Basin, whereas the Nansen Basin presents values as high as 58.9 nmol L^{-1}.

N_2O concentrations (Fig. 4f) ranged between 6.9 and 18.2 nmol L^{-1} (42–111% saturation, relative to the atmospheric concentration). N_2O distribution showed a slight oversaturation of up to 111% in the Amundsen Basin, whereas under-saturated waters at around 50–70% were present in the Nansen Basin. Below the PML, N_2O values remained fairly constant throughout the water column up to 100 m depth, with levels between under-saturation (40–90%) and at equilibrium with the atmosphere (100%). In contrast, CH_4 strongly fluctuated between 1.0 and 23.9 nmol L^{-1} (27–649% saturation) in the PML and the halocline (Fig. 4g). CH_4 oversaturation was primarily observed within the first 100 m depth, except for some stations where levels were almost in equilibrium with the atmosphere.

Fig. 5 illustrates the cross section in the distributions of biogeochemical variables from 100 to 900 m depth associated with AIW. NO_3^- and PO_4^{3-} (Fig. 5a; c) varied between 1.1 and 17.2 and between 0.9 and 1.6 μmol L^{-1}, respectively (similar to surface waters) and these values increased with water depth. NO_3^- and PO_4^{3-} profiles showed higher values at the northward and southward ends of the transect, as high as 15.0 and 1.6 μmol L^{-1}, respectively, with decreasing values in the middle of the transect (ST 2, 9, 10 and 1), i.e. NO_3^- concentrations < 10.0 μmol L^{-1}. PO_4^{3-} profiles remained constant in the AIW. NO_2^- concentration (Fig. 5b) varied between zero to 0.2 μmol L^{-1} (similar to surface waters) and remained uniform in the AIW. N/P ratio (Fig. 5d) varied between 7.5 and 12.5 (higher values than in surface waters). Lower values (~7.5) were observed in the middle of the SNT (ST 2, 8, 9, 10 and 1).

N_2O concentration and saturation levels (Fig. 5e) varied between 10.0 and 16.0 nmol L^{-1} and from 68% (under-saturated level) to 111% (slightly saturated), respectively. This is similar to the levels found in surface waters, which were similar in both basins, except at ST 9 and ST 10 (Nansen Basin) where values as low as 68% saturation were found. CH_4 concentration and saturation levels (Fig. 5f) varied between 1.0-11.1 nmol L^{-1} and 29–329%, respectively, which is lower than the values observed in the surface waters. The Amundsen Basin remained under-saturated in CH_4 (30–90%) and the Nansen Basin was saturated by up to 250%.

Fig. 6 shows the distribution of biogeochemical variables between 900 and 4300 m depth (ADW). NO_3^- profiles (Fig. 6a) showed higher concentrations at ST 1 (~15 μmol L^{-1}), in the northern sector of the Nansen Basin; and at ST 5, 3 and 2 in the Amundsen Basin (~15-17.5 μmol L^{-1}). A maximum of 17.5 μmol L^{-1} was reached near-bottom in both basins. NO_2^- concentrations (Fig. 6b) reached lows of 0–0.2 μmol L^{-1} and remained constant within ADW, with slightly lower concentrations than AIW. The southward stations (ST 1, 11 and 12) were an exception to this, where the AIW intrusion was apparent and increased concentrations of around 1.5 μmol L^{-1} occurred. PO_4^{3-} distribution (Fig. 6c) remained similar in both basins, with concentrations of around 1.5 μmol L^{-1}, except for ST 1, where lower PO_4^{3-} concentrations were found (~1.2 μmol L^{-1} below 1500 m depth, Fig. 6c). The N/P ratio (Fig. 6d) exhibits different values in both basins, with higher values in the Amundsen (between 10.0 and 12.5) compared to the Nansen Basin (< 10).

N_2O concentrations (Fig. 6e) ranged between 8.0 and

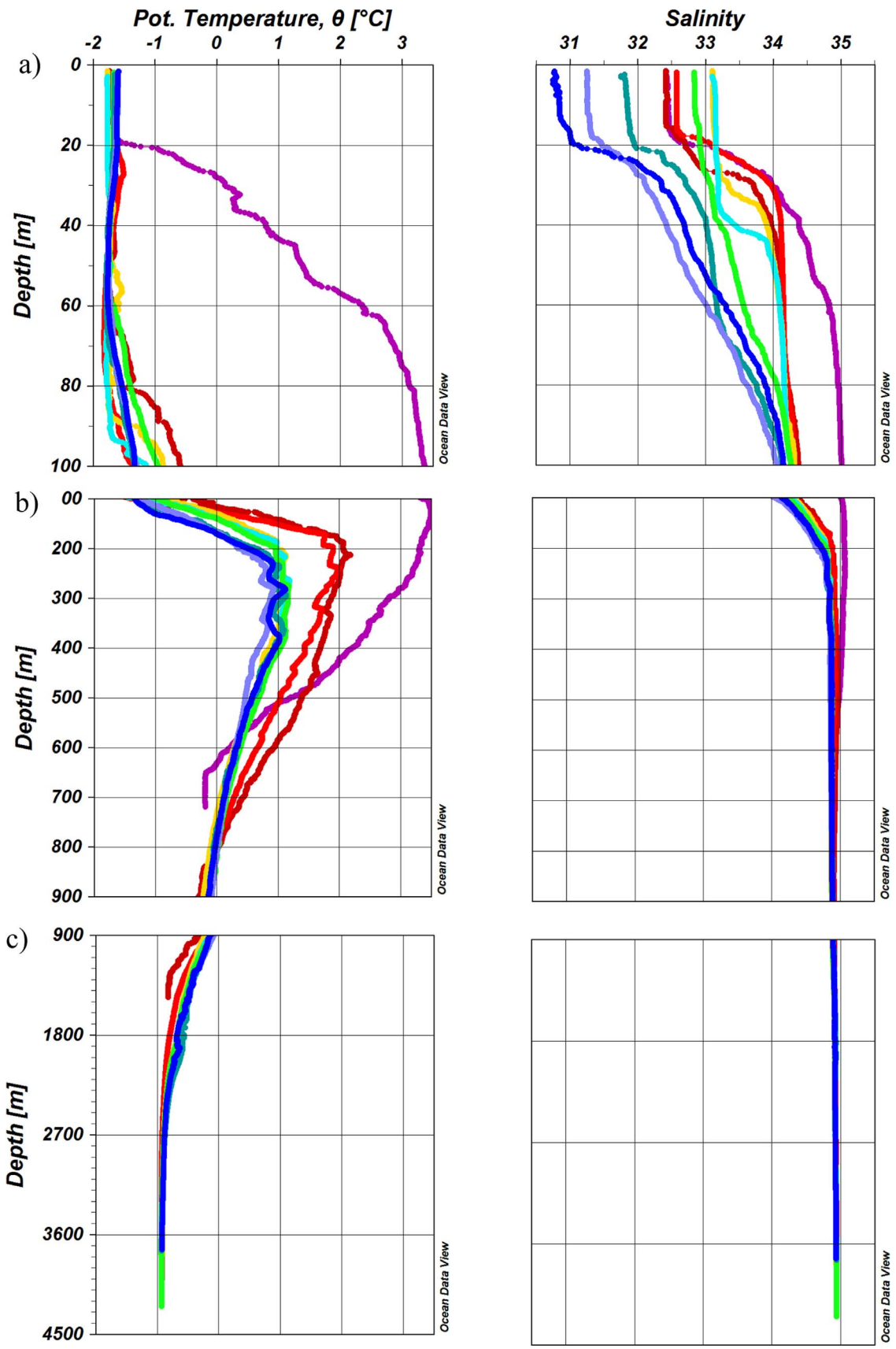

Fig. 3. Vertical profiles of potential temperature and salinity of a) Polar Mixed Layer and halocline (0–100 m); b) Atlantic Intermediate Water (100–900 m) and c) Arctic Deep Water (900–4300 m). Colour stations are the same of global map from Fig. 2.

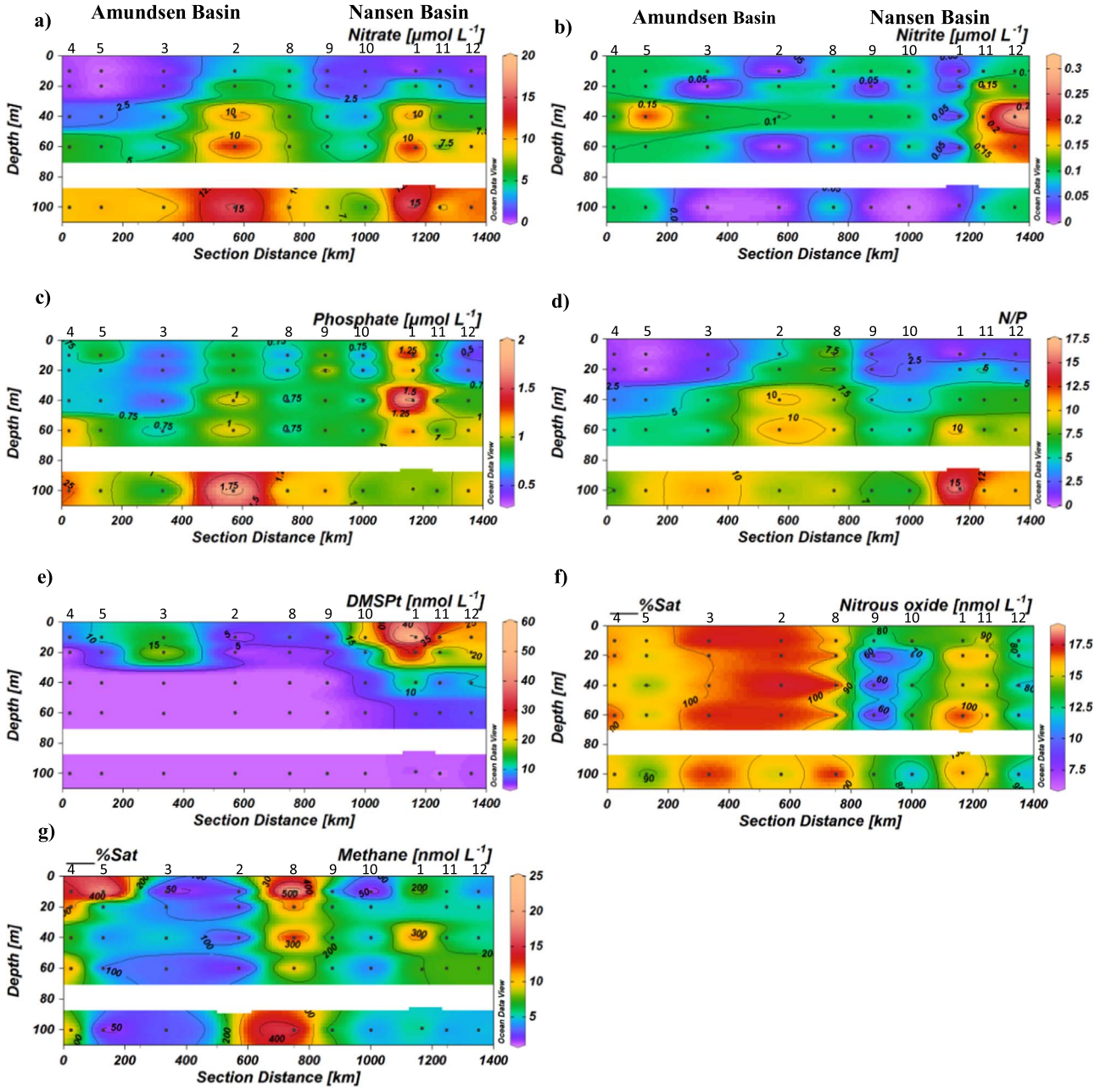

Fig. 4. Vertical cross section for PML and halocline (0–100 m depth) of a) nitrate (µmol L^{-1}); b) nitrite (µmol L^{-1}); c) phosphate (µmol L^{-1}); d) N/P ratio; e) DMSPt (nmol L^{-1}); f) nitrous oxide (nmol L^{-1}, % saturation); and g) methane (nmol L^{-1}, % saturation), across the SNT. Dots indicate sample position.

16.1 nmol L^{-1} (52–106% saturation in relation to the atmospheric equilibrium concentration), similar to PML, the halocline and AIW. N_2O distribution in both basins was homogenous and values remained slightly under-saturated (80–90%) in the water column up to 4300 m depth. In contrast, CH_4 (Fig. 6f) fluctuated sharply between 1 and 11.8 nmol L^{-1} (28%-340% saturation), which are lower concentrations than in PML and the halocline. CH_4 oversaturation (as high as 340%) occurred mostly up to 4300 m depth, except for ST 5 (50% saturation below 2000 m) and ST 2 (51–100%) in the Amundsen Basin.

4. Discussion

4.1. Regional settings

The water column was highly stratified between the surface and 100 m depth (PML and halocline), a feature that hinders mixing and slows the exchange of nutrients and gases between the surface and the underlying water masses. Low salinities at the surface immediately below the sea ice cap may be a consequence of several processes, including sea ice melting cycles; inflow of water from the Pacific Ocean via the Bering Strait, which is fresher than the North Atlantic waters (Jones et al., 2008); and continental runoff primarily from the Siberian shelves (Björk et al., 2002). In our study, the halocline caused pronounced stratification, which varied due to the thaw-freeze cycle of sea ice and important freshwater inputs (Carmack and Wassmann, 2006). The PML and halocline formed a strong physical barrier in the water column, capable of insulating surface ice cover from subsurface layers by limiting upward heat flux (Aagaard and Carmack, 1989). The formation of sea ice over the continental shelf produces cold, brine-enriched waters that flow off the shelf into the central regions of the Arctic Ocean, resulting in a cold and saline halocline (Aagaard et al., 1981; Rudels et al., 1996). This is maintained by large-scale lateral advection from certain sections of the broad continental shelf which borders the Polar Basin (Aagaard et al., 1981).

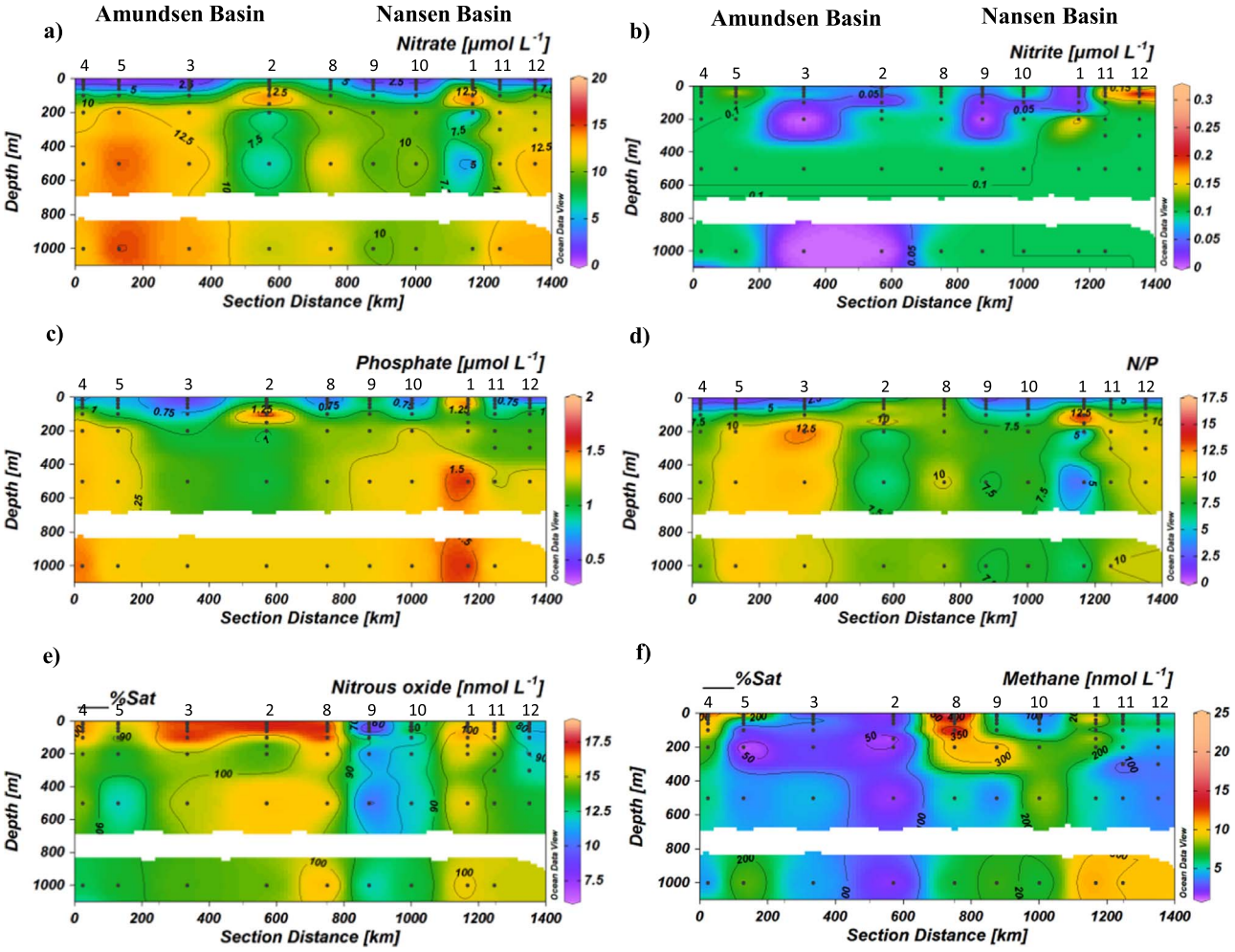

Fig. 5. Vertical cross section for Atlantic Intermediate Water (100–900 m depth) of a) nitrate (µmol L^{-1}); b) nitrite (µmol L^{-1}); c) phosphate (µmol L^{-1}); d) N/P ratio; e) nitrous oxide (nmol L^{-1}, % saturation); and f) methane (nmol L^{-1}, % saturation), across the SNT. Dots indicate sample position.

Differences in temperature and salinity were observed at the PML and halocline between the Nansen and Amundsen Basins, as shown in Fig. 3a. The stations closer to the north (Amundsen Basin) were fresher and colder, in contrast with the southern stations (Nansen Basin), which were saltier and warmer. The latter could be due to the influence of Pacific derived waters (Pdw) from the north (0–50 m) and Adw from the south (Jones et al., 2003). The influence of Adw is clearly shown at ST 12 (Fig. 3a). This water mass enters through the Fram Strait (between Greenland and Svalbard) and through the Barents Sea, as previously reported by Jones (2001) and Rudels et al. (2013).

In addition, the observed differences in oceanographic features of AIW and ADW between the Nansen and Amundsen Basins (see Fig. 3b; c) were propagated by long residence times due to restricted circulation and exchange within the Eurasian Basin. In effect, AIW enters the Arctic Ocean through the Barents Sea and the Fram Strait, which are the only passages that allow the exchange of deep water in this region (Jones et al., 1995). The overturning of the intermediate and deep waters in the Arctic Ocean play a key role in global circulation and climate moderation (Swift et al., 1983), and strongly influence the water mass structure in terms of nutrients and gases distributions, as revealed in this study.

4.2. Distribution of biogeochemical variables

4.2.1. PML and halocline

Vertical nutrient distribution showed a consistent pattern, in agreement with biological consumption and remineralization, and advection processes in the study area. Nutrient depletion near the surface is observed during each summer period, when the light limitation decreases and the sea ice breaks up, allowing phytoplankton blooms to spread along the base of the sea ice (Arrigo et al., 2012). Remarkably, surface N/P ratios were low in both basins and never reached the expected Redfield ratio (16/1) (Fig. 4d). In effect, NO_3^- became limiting before the exhaustion of PO_4^{3-}, indicating the existence of previously mentioned P-excess in the system (Yamamoto-Kawai et al., 2006; Hawkings et al., 2016). One of the most plausible origins of this PO_4^{3-} excess is the glaciers from Greenland. The physical erosion of bedrock exposes ground apatite to biogeochemical weathering ultimately liberating PO_4^{3-} to the Arctic Ocean. Hawkings et al. (2016) suggested that the Greenland Ice Sheets are the region of most efficient P weathering and export of PO_4^{3-} to surrounding regions, and that the export of dissolved phosphorous could equal that of the largest rivers in the world, like the Mississippi and the Amazon.

In this study, the N/P ratio was strongly modified in the surface waters. This is likely to have been induced by a shift from new to regenerated production (Damm et al., 2015), as melting sea ice is known to release NH_4^+, alleviating NO_3^- limitation (Tovar-Sánchez et al., 2010). During the sea ice melting season, light penetration strongly decreases due to sinking particles and microalgae released from the sea ice (Mundy et al., 2005). This pattern may stimulate bacteria/archaea activity (Galindo et al., 2014).

High surface CH_4 saturation was identified at almost all sample stations down to 100 m depth (Fig. 4g), indicating a strong potential for CH_4 production in these water masses, and for CH_4 effluxes that

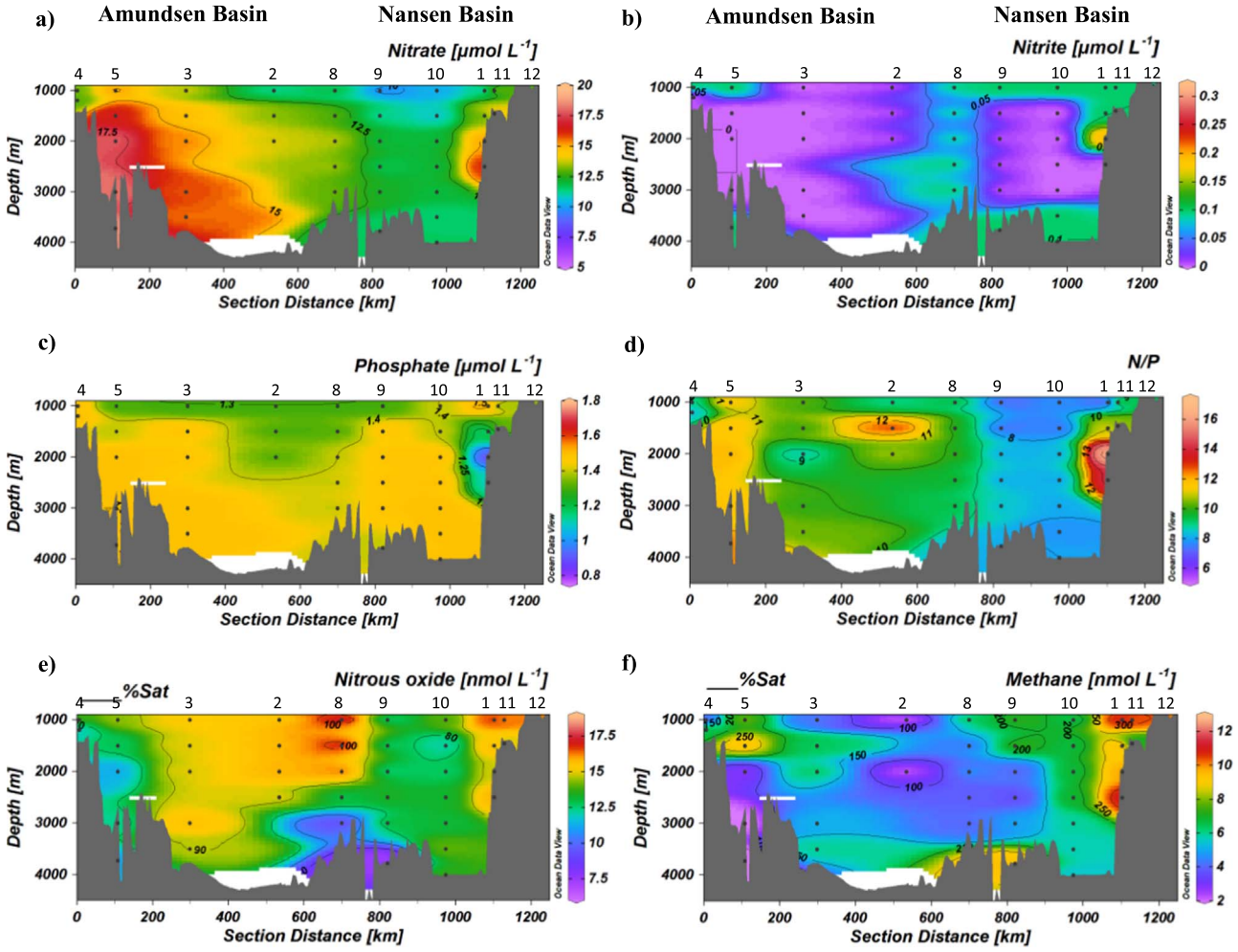

Fig. 6. Vertical cross section for Arctic Deep Water (900–4300 m depth) of a) nitrate (µmol L^{-1}); b) nitrite (µmol L^{-1}); c) phosphate (µmol L^{-1}); d) N/P ratio; e) nitrous oxide (nmol L^{-1}, % saturation); and f) methane (nmol L^{-1}, % saturation), across the SNT. Dots indicate sample position.

could occur if the sea ice retreat continues at current rates. Interestingly, several surface stations (ST 4, 5, 8 and 1) displayed CH_4 saturation levels as high as 650%. Although it remains unclear at present how CH_4 is formed in sea ice, it is possible that CH_4 could be produced via the methylotrophic pathway mediated by methylated compounds (Schäfer, 2007; Sun et al., 2011). One candidate for methylated compounds is DMSP and/or DMS, as indicated in the surface water by Damm et al. (2010) and Florez-Leiva et al. (2013). This assumption is supported by the extensive production of DMSP, a precursor for CH_4 production, which is produced as an osmolyte, or cryoprotectant by sea ice algae during primary production in the sea ice (Kirst et al., 1991; Levasseur et al., 1994). $DMSP_t$ concentrations under the sea ice in the Nansen Basin are higher than in the Amundsen Basin (Fig. 4e), and the same pattern is observed for CH_4. This may suggest that the microalgal activities involved in DMSP cycling at the base of the sea ice may be linked with CH_4 generation. Oceanic surface waters are systematically supersaturated with CH_4, once known as the methane paradox (Lamontagne et al., 1973). This situation persists in Open Ocean far away of anoxic sediments, where anaerobic organic matter respiration and CH_4 formation are expected (methanogenesis). However, suspended particles, zooplankton biomass and freshly defecated fecal pellets have been examined as possible sources for CH_4 production in oxygenated seawater (Karl and Tillbrook, 1994; Marty et al., 2001; Karl et al., 2008). Some studies have shown the presence of methanogenic microorganisms in these particles and have suggested that methanogenic activity originates in the digestive tracts of zooplankton and in fecal pellets. Below the ice pack, subsurface peaks of phytoplankton biomass persist, called the subsurface chlorophyll maxima (Arrigo et al., 2011), which has recently been described as an important site for predator–prey interactions (Scott et al., 2010). Thus, the existence of an abundant and active zooplankton community (including protozooplankton), and therefore pellet production (Hirche and Mumm, 1992; Morata and Seuthe, 2014), may also support anaerobic methanogenesis, playing a critical role in trophic coupling.

With regards to N_2O levels, this gas showed a wide range of concentrations from under-saturation to light oversaturation in surface waters (see Fig. 4f). It is likely that this is produced by nitrifying activity since nitrification is an ubiquitous process that occurs in all oceans, even in cold and nutrient depleted Arctic waters (Shiozaki et al., 2016) and Antarctic coastal waters (Tolar et al., 2016). Therefore, active nitrification mediated by microbes under the sea ice could be occurring, oxidizing NH_4^+ and producing N_2O as a byproduct of this reaction, especially bearing in mind that sea ice melt can release NH_4^+ (Tovar-Sánchez et al., 2010). Indeed, previous experiments in the coastal Arctic Ocean have shown the presence of ammonia-oxidizing Betaproteobacteria and Crenarchaea, and potentially high nitrification rates with higher values in the winter compared with the summer, due to competition with phytoplankton for NH_4^+ concentrations (Christman et al., 2011).

Under-saturation of N_2O may result from water intrusions from sea ice melt (with a low gas content), that dilutes the surrounding water mass. This pattern has been previously reported in the Arctic Ocean (Kitidis et al., 2010; Randall et al., 2012), and is subsequently affected by mixing processes and water mass circulation. Under-saturation of

N_2O has also been described in the Bering Sea and the Indian Sector of the Southern Ocean (Chen et al., 2014; Farías et al., 2015). However, physical processes are probably not the only processes producing those very under-saturated levels. Canonical denitrification consumes N_2O during its dissimilative reduction to N_2, but given that this pathway occurs at suboxic-anoxic levels (Bange et al., 2010) it is precluded in oxygenated water, unless it takes place in suboxic-anoxic microsites (Klawonn et al., 2015). We cannot discard that denitrification could take place at the base of the sea ice, especially considering the fact that during freezing periods, salts and gases (O_2, N_2O, CH_4) are expelled from sea ice and the low O_2 conditions generated may induce denitrification (Loose et al., 2009; Randall et al., 2012). Little is known about N_2O cycling in intermediate and deep waters, and it is presumed to be negligible in the Arctic Ocean (by nitrification and denitrification) according to indirect estimates (Freing et al., 2012).

In recent years, it has become apparent that nitrogen fixation is not restricted to the (sub) tropical and oligotrophic marine regions, but that there is also potential for diazotrophic activity in Arctic waters (Díez et al., 2012). Also, the diazotrophic community may be dominated by heterotrophic bacteria (Farnelid et al., 2011, 2013; Moisander et al., 2014; Bentzon-Tilia et al., 2015). In this study, significant N_2 and N_2O fixation rates were determined in surface waters and in ice brine during the same expedition cruise. ^{15}N-N_2O tracer experiments showed very high consumption rates for treatments with $^{15}N_2O$-DMS and $^{15}N_2O$-HCO_3^- of 185 ± 99 and 105 ± 27 nmol L^{-1} d^{-1}, respectively (Snoeijs unpublished data). The ^{15}N-N_2 experiments were also positive at most of the sampling stations, indicating new input of N into the system, which may support the hypothesis that N_2 fixation is an extremely versatile process, being led by both autotrophic (Cyanobacteria) and heterotrophic bacteria in Arctic Ocean brine and seawater. Thus, the existence of N-fixing microorganisms in this marine region may have an effect on the N_2O inventory, which could be used as an alternative substrate, as suggested by Farías et al. (2013). Microorganisms that carry out biological N_2O fixation could produce N_2O depletion and simultaneous under-saturation in these marine environments. Thus, N_2O depletion in the Arctic might partially be explained by N-fixation, which has been suggested in Arctic surface waters; biological N_2O fixation offers a very plausible explanation, given the observed N/P ratio, and could be stimulated when NO_3^- is limiting but PO_4^{3-} is not (Jones et al., 2003).

4.2.2. AIW and ADW

In terms of the physical processes in intermediate and deep waters, the long residence times of water in the Eurasian Basin is due to the highly restricted exchange of water with the surrounding oceans (Rudels et al., 2013). Also, the Fram Strait has a sill depth of ~2500 m, so Arctic Bottom Water from the Eurasian Basin has an isolation age of 250 years (Schlosser et al., 1997). These mechanisms should strongly modify the distribution of greenhouse gases and nutrients in the EAB. In fact, waters from the Amundsen Basin are older than those of the Nansen Basin as a result of this physical mechanism. This was also taken into account when N_2O saturation was estimated with the atmospheric preindustrial value of 270 ppb (Battle et al., 1996). N_2O under-saturation level still remains, especially in the Amundsen Basin with 13–15% difference between current and pre-industrial times. The Amundsen Basin has more nutrient content produced by the remineralization of organic matter and N/P values are closer to the expected Redfield ratio (Figs. 5 and 6), and also reach lower gas concentrations probably associated with some biogenic consumption.

Differences in the distributions and concentrations of CH_4 were also observed in both basins, with CH_4 under-saturation (28–100%) in the Amundsen Basin and oversaturation in the Nansen Basin (> 100%). Potentially, part of the CH_4 oversaturation in AIW and ADW in the Nansen Basin comes from cold seeps in the subsurface layers of the continental margin of Svalbard (Westbrook et al., 2009; Steinle et al., 2015). There is evidence for most of this gas coming from thermogenic sources in the Vestnesa Ridge (Fram Strait) in the form of gas-hydrates (Smith et al., 2014). This ecosystem in known to contains large amounts of CH_4 in the form of solid gas hydrates, gaseous reservoirs or dissolved gas in pore waters (Wallmann et al., 2012), which may ascend from the sea floor and be available to anaerobic and aerobic methanotrophic microbes (Knittel and Boetius, 2009; Boetius and Wenzhöfer, 2013). In contrast, the low levels of CH_4 found in the Amundsen Basin may be related to CH_4 oxidation through methanotrophic activity. In fact, Heintz et al. (2012) showed that methane oxidation rates below 700 m in the Santa Monica Basin were between 0.12 and 1.35 nmol L^{-1} d^{-1}. Aerobic CH_4 oxidation is known to be performed by methanotrophic bacteria (MOB), typically belonging to the Gamma- (type I) or Alphaproteobacteria (type II) (Hanson and Hanson, 1996; Murrell, 2010). The metabolic activity of these microorganisms may therefore cause CH_4 under-saturation in the Amundsen Basin. Indeed, molecular analyses derived from 16S itags Illumina sequencing, from surface ice brine and seawater underneath the sea ice, during the same cruise, revealed that Gammaproteobacteria *Methylococcus capsulatu* was the most abundant methanotroph in this region (Díez, unpublished data). CH_4 under-saturation has been previously described in intermediate and deep waters of the northern Atlantic (Scranton and Brewer, 1978) and in Baffin Bay Deep Water, in which the authors found CH_4 concentrations as low as 0.20 nmol L^{-1} (6% saturation) and they attributed those low levels to microbial oxidation (Punshon et al., 2014). In this study, CH_4 levels are also coincident with the increasingly restricted circulation of bottom waters in the Eurasian Basin.

Due to the direct connection between the EAB and the North Atlantic Ocean via the Fram Strait, we propose that part of the gas content is likely to come from intermediate and deep waters. N_2O distribution in intermediate and deep waters is poorly known (no data have been reported so far to the best of our knowledge), so any processes involved in N_2O cycling are merely speculative. In spite of the lack information on the N_2O distribution, Atlantic Meridional Transect (AMT) programme (from UK) has allowed the measurement and collection of N_2O between 50°N and 52°S. This transect crossed a total of 7 biogeographical provinces defined by Longhurst (1998), being the North Atlantic Drift (NADR, 44–58°N) the closest province to the Arctic Ocean (Eurasian Basin). N_2O levels in this province have been reported to be lightly under-saturated with values of 98% saturation and around 7.6 nmol L^{-1} in the mixing layer (Forster et al., 2009). Finally, it may be possible that water masses forming in this area are deplete in N_2O which in turn influences N_2O content of the EAB (Freing et al., 2012).

However, N_2O under-saturation as low as 52% has been registered. Biological processes promoting that N_2O under-saturation could be associated with denitrification or N_2O fixation as was mentioned. In contrast to the surface layer, neither N_2O nor N_2 fixation was measured in the AIW or ADW, so the existence of these processes cannot be supported. Total denitrification was not measured in the Eurasian Basin, but given that the AIW and ADW are oxygenated, this process would only be possible in sediments or in microsites (particles).

5. Concluding remarks

The heterogeneous distribution of greenhouse gases and $DMSP_t$ was observed in the PML and the halocline of the Arctic Ocean, revealing a strong oversaturation of CH_4 (120–649%) and high $DMSP_t$ levels (up to 58.9 nmol L^{-1}), particularly in the Nansen Basin; while N_2O displayed sub- to slightly saturated conditions 90–111%) along the SNT. In the AIW, N_2O remained variable but with low concentrations (70–110%); whereas CH_4 presented oversaturation levels (up to 330%) in the Nansen Basin, but strong under-saturation (30% saturation) in the Amundsen Basin. In AIW and ADW, N_2O show slightly oversaturated levels in Amundsen Basin, but under-saturated levels in

Nansen Basin in contrast to CH_4, that show strongly oversaturated levels in Nansen Basin but under-saturated levels in Amundsen Basin possibly attributed to the effect of overturning water mass circulation. Two important aspects must be considered when observing greenhouse gas content in cold waters: in the surface layer, the freezing-melting cycles and biological effects are crucial for vertical and spatial gas distribution; and in intermediate and deep waters, the residence times of deep water circulation and thermogenic processes may determine the concentrations of these climatically active gases. Nutrient concentrations increased with water depth, reaching N/P values of around 12.5 (lower than expected according to the Redfield ratio), indicating the remineralization of organic matter. The N/P ratio differed between the basins, with higher levels in the Amundsen compared with the Nansen Basin, according to the age of the water masses. This research reports greenhouse gas distribution in PML and halocline, as well as AIW and ADW, and is one of the first known publications on this subject. This study is particularly relevant because Arctic sea ice cover is decreasing at a faster rate than previously forecast. In fact, during 2012 when the LOMROG III cruise took place, Arctic sea ice extent had dropped to a new record low, twice as low as the 1979–2000 minimum average, covering only 3.39 million km^2 (Perovich et al., 2012). Investigating the potential biogeochemical consequences of this is therefore of vital importance.

Acknowledgements

This work was supported by the Swedish Research Foundation VR (Research Infrastructures SWEDARCTIC 2011–2015), the Swedish Research Foundation FORMAS (Project 2012-1459) and the Carl Trygger Foundation for Scientific Research (2012) to PS. The assistance from the Swedish Polar Research Secretariat in practical matters before and during the cruise is acknowledged. JV received a scholarship from CONICYT (Master's Program in Chile) and INACH (MT_02-13). LF funded the analysis of samples obtained during the LOMROG cruise with FONDECYT N° 1120719. BD funded travel to the Arctic and further data analysis with INACH10-15 project. Sea ice concentration data from DATE to DATE were obtained from http://www.meereisportal.de (grant: REKLIM-2013-04, BMBF), and we acknowledge Marcel Nicolaus for his support with the sea ice map. This is a contribution by 15110009 (FONDAP CR^2-CONICYT).

References

Aagaard, K., Carmack, E.C., 1989. The role of sea ice and other fresh water in the Arctic circulation. J. Geophys. Res.: Oceans 94, 14485–14498. http://dx.doi.org/10.1029/JC094iC10p14485.

Aagaard, K., Coachman, L.K., Carmack, E., 1981. On the halocline of the Arctic Ocean. Deep Sea Res. Part A 28, 529–545. http://dx.doi.org/10.1016/0198-0149(81)90115-1.

Anderson, L.G., Falck, E., Jones, E.P., Jutterström, S., Swift, J.H., 2004. Enhanced uptake of atmospheric CO_2 during freezing of seawater: a field study in Storfjorden, Svalbard. J. Geophys. Res.: Oceans 109, C06004. http://dx.doi.org/10.1029/2003JC002120.

Arrigo, K.A., Dijken, G.V., Pabi, S., 2008. Impact of a shrinking Arctic ice cover on marine primary production. Geophys. Res. Lett. 35, L19603. http://dx.doi.org/10.1029/2008GL035028.

Arrigo, K.R., Matrai, P.A., van Dijken, G.L., 2011. Primary productivity in the Arctic Ocean: impacts of complex optical properties and subsurface chlorophyll maxima on large-scale estimates. J. Geophys. Res. 116, C11022. http://dx.doi.org/10.1029/2011JC007273.

Arrigo, K.R., Perovich, D.K., Pickart, R.S., Brown, Z.W., Dijken, G.L., Van, Lowry, K.E., Mills, M.M., Palmer, M.A., Balch, W.M., Bahr, F., Bates, N.R., Benitez-Nelson, C., Bowler, B., Brownlee, E., Ehn, J.K., Frey, K.E., Garley, R., Laney, S.R., Lubelczyk, L., Mathis, J., Matsuoka, A., Mitchell, B.G., Moore, G.W.K., Ortega-Retuerta, E., Pal, S., Polashenski, C.M., Reynolds, R.A., Schieber, B., Sosik, H.M., Stephens, M., Swift, J.H., 2012. Massive phytoplankton blooms under Arctic Sea Ice. Science 336, 1408. http://dx.doi.org/10.1126/science.1215065.

Bange, H.W., Freing, A., Kock, A., Löscher, C.R., 2010. Marine pathways to nitrous oxide. In Nitrous oxide and climate change (ed. Smith K.), pp. 36–62 London, UK: Earthscan

Battle, M., Bender, M., Sowers, T., Tans, P.P., Butler, J.H., Elkins, J.W., Ellis, J.T., Conway, T., Zhang, N., Lang, P., Clarke, A.D., 1996. Atmospheric gas concentrations over the past century measured in air from firn at the South Pole. Nature 383, 231–235. http://dx.doi.org/10.1038/383231a0.

Bentzon-Tilia, M., Traving, S.J., Mantikci, M., Knudsen-Leerbeck, H., Hansen, J.L.S., Markager, S., Riemann, L., 2015. Significant N_2 fixation by heterotrophs, photoheterotrophs and heterocystous cyanobacteria in two temperate estuaries. Int. Soc. Microb. Ecol. 9, 273–285. http://dx.doi.org/10.1038/ismej.2014.119.

Björk, G., Söderkvist, J., Winsor, P., Nikolopoulos, A., Steele, M., 2002. Return of the cold halocline layer to the Amundsen Basin of the Arctic Ocean: implications for the sea ice mass balance. Geophys. Res. Lett. 29, 8–1-8-4. http://dx.doi.org/10.1029/2001GL014157.

Boetius, A., Wenzhöfer, F., 2013. Seafloor oxygen consumption fuelled by methane from cold seeps. Nat. Geosci.: Rev. 6, 725–734. http://dx.doi.org/10.1038/ngeo1926.

Carmack, E., Wassmann, P., 2006. Food webs and physical–biological coupling on pan-Arctic shelves: unifying concepts and comprehensive perspectives. Prog. Oceanogr. 71, 446–477. http://dx.doi.org/10.1016/j.pocean.2006.10.004.

Chen, L., Gao, Z., Sun, H., Chen, B., Cai, W., 2014. Distributions and air-sea fluxes of CO_2 in the summer Bering Sea. Acta Oceanol. Sin. 33, 1–8. http://dx.doi.org/10.1007/s13131-014-0483-9.

Christman, G., Cottrell, M.T., Popp, B.N., Gier, E., Kirchman, D.L., 2011. Abundance, diversity, and activity of ammonia-oxidizing prokaryotes in the coastal Arctic Ocean in Summer and Winter. Appl. Environ. Microbiol. 77, 2026–2034. http://dx.doi.org/10.1128/AEM.01907-10.

Codispoti, L.A., Christensen, J.P., 1985. Nitrification, denitrification and nitrous oxide cycling in the eastern tropical South Pacific Ocean. Mar. Chem. 16, 277–300. http://dx.doi.org/10.1016/0304-4203(85)90051-9.

Comiso, J.C., 2010. Fundamental Characteristics of the Polar Oceans and Their Sea Ice Cover, in: polar Oceans from Spac. In: Mysak, L.A., Hamilton, K. (Eds.), Atmospheric and Oceanographic Sciences Library 41, 19–79. http://dx.doi.org/10.1007/978-0-387-68300-3.

Cornejo, M., Murillo, A.A., Farías, L., 2015. An unaccounted for N_2O sink in the surface water of the eastern subtropical south Pacific: physical versus biological mechanisms. Prog. Oceanogr. Part A 137, 12–23. http://dx.doi.org/10.1016/j.pocean.2014.12.016.

Crutzen, P.J., 1991. Methane's sinks and sources. Nature 350, 380–381. http://dx.doi.org/10.1038/350380a0.

Damm, E., Helmke, E., Thoms, S., Schauer, U., Nöthig, E., Bakker, K., Kiene, R.P., 2010. Methane production in aerobic oligotrophic surface water in the central Arctic Ocean. Biogeosciences 7, 1099–1108. http://dx.doi.org/10.5194/bg-7-1099-2010.

Damm, E., Rudels, B., Schauer, U., Mau, S., Dieckmann, G., 2015. Methane excess in Arctic surface waters- triggered by sea ice formation and melting. Sci.: Rep. 5, 16179. http://dx.doi.org/10.1038/srep16179.

Díez, B., Bergman, B., Pedrós-Alió, C., Antó, M., Snoeijs, P., 2012. High cyanobacterial nifH gene diversity in Arctic seawater and sea ice brine. Environ. Microbiol. Rep. 4, 360–366. http://dx.doi.org/10.1111/j.1758-2229.2012.00343.x.

Elkins, J.W., Wofsy, S.C., McElroy, M.B., Kolb, C.E., Kaplan, W.A., 1978. Aquatic sources and sinks for nitrous oxide. Nature 275, 602–606. http://dx.doi.org/10.1038/275602a0.

Farías, L., Fernández, C., Faúndez, J., Cornejo, M., Alcaman, M.E., 2009. Chemolithotrophic production mediating the cycling of the greenhouse gases N_2O and CH_4 in an upwelling ecosystem. Biogeosciences 6, 3053–3069. http://dx.doi.org/10.5194/bg-6-3053-2009.

Farías, L., Faúndez, J., Fernández, C., Cornejo, M., Sanhueza, S., Carrasco, C., 2013. Biological N_2O fixation in the Eastern South Pacific Ocean and marine cyanobacterial cultures. PLoS ONE 8, e63956. http://dx.doi.org/10.1371/journal.pone.0063956.

Farías, L., Florez-Leiva, L., Besoain, V., Sarthou, G., Fernández, C., 2015. Dissolved greenhouse gases (nitrous oxide and methane) associated with the naturally iron-fertilized Kerguelen region (KEOPS 2 cruise) in the Southern Ocean. Biogeosciences 12, 1925–1940. http://dx.doi.org/10.5194/bg-12-1925-2015.

Farnelid, H., Andersson, A.F., Bertilsson, S., Al-Soud, W.A., Hansen, L.H., Sørensen, S., Steward, G.F., Hagström, A., Riemann, L., 2011. Nitrogenase gene amplicons from global marine surface waters are dominated by genes of non-cyanobacteria. PLoS ONE 6, e19223. http://dx.doi.org/10.1371/journal.pone.0019223.

Farnelid, H., Bentzon-Tilia, M., Andersson, A.F., Bertilsson, S., Jost, G., Labrenz, M., Jürgens, K., Riemann, L., 2013. Active nitrogen-fixing heterotrophic bacteria at and below the chemocline of the central Baltic Sea. Int. Soc. Microb. Ecol. 7, 1413–1423. http://dx.doi.org/10.1038/ismej.2013.26.

Florez-Leiva, L., Damm, E., Farías, L., 2013. Methane production induced by dimethylsulfide in surface water of an upwelling ecosystem. Prog. Oceanogr. 112–113, 38–48. http://dx.doi.org/10.1016/j.pocean.2013.03.005.

Forster, G., Upstill-Goddard, R., Gist, N., Robinson, C., Uher, G., Woodward, E.M.S., 2009. Nitrous oxide and methane in the Atlantic Ocean between 50 °N and 52 °S: latitudinal distribution and sea-to-air flux. Deep Sea Res. II 56, 964–976. http://dx.doi.org/10.1016/j.dsr2.2008.12.002.

Foster, R.A., Paytan, A., Zehr, J.P., 2009. Seasonality of N_2 fixation and nifH gene diversity in the Gulf of Aqaba (Red Sea). Limnol. Oceanogr. 54, 219–233. http://dx.doi.org/10.4319/lo.2009.54.1.0219.

Freing, A., Wallace, D.W.R., Bange, H.W., 2012. Global oceanic production of nitrous oxide. Philos. Trans. R. Soc. 367, 1245–1255. http://dx.doi.org/10.1098/rstb.2011.0360.

Galindo, V., Levasseur, M., Mundy, C.J., Gosselin, M., Tremblay, J.-E., Scarratt, M., Gratton, Y., Papakiriakou, T., Poullin, M., Lozotte, M., 2014. Biological and physical processes influencing sea ice, under-ice algae, and dimethylsulfoniopropionate during spring in the Canadian Arctic Archipelago. J. Geophys. Res.: Oceans, 119. http://dx.doi.org/10.1002/2013JC009497.

Gleitz, M., Rutgers van der Loeff, M., Thomas, D.N., Dieckmann, G.S., Millero, F.J., 1995. Comparison of summer and winter inorganic carbon, oxygen and nutrient concentration in Antarctic sea ice brine. Mar. Chem. 51, 81–91. http://dx.doi.org/10.1016/0304-4203(95)00053-T.

Hanson, R.S., Hanson, T.E., 1996. Methanotrophic bacteria. Microbiol. Rev. 60, 439–471.

Hawkings, J., Wadham, J., Tranter, M., Telling, J., Bagshaw, E., Beaton, A., Simmons, S.-L., Chandler, D., Tedstone, A., Nienow, P., 2016. The Greenland Ice Sheet as a hot spot of phosphorus weathering and export in the Arctic. Glob. Biogeochem. Cycles

30, 191–210. http://dx.doi.org/10.1002/2015GB005237.
Heintz, M.B., Mau, S., Valentine, D.L., 2012. Physical control on methanotrophic potential in waters of the Santa Monica Basin. Limnol. Oceanogr. 57, 420–432. http://dx.doi.org/10.4319/lo.2012.57.2.0420.
Herrero, A., Muro-Pastor, A.M., Flores, E., 2001. Nitrogen control in cyanobacteria. J. Bacteriol. 183, 411–425. http://dx.doi.org/10.1128/JB.183.2.411-425.2001.
Hirche, H.-J., Mumm, N., 1992. Distribution of dominant copepods in the Nansen Basin, Arctic Ocean, in summer. . Deep Sea Res. Part A 39, S485–S505. http://dx.doi.org/10.1016/S0198-0149(06)80017-8.
IPCC, 2014. Climate Change 2014: Mitigation of Climate Change. Contribution of Working Group III to the Fifth Assessment Report of the Intergovernmental Panel on Climate Change. Edenhofer, O., Pichs-Madruga, R., Sokona, Y., Farahani, E., Kadner, S., Seyboth, K., Adler, A., Baum, I., Brunner, S., Eickemeier, P., Kriemann, B., Savolainen, J., Schlömer, S., von Stechow, C., Zwickel, T., Minx J.C. (Eds). Cambridge University Press, Cambridge, United Kingdom and New York, NY, USA.
Jones, E.P., Rudels, B., Anderson, L.G., 1995. Deep waters of the Arctic Ocean: origins and circulation. . Deep Sea Res. Part I 42, 737–760. http://dx.doi.org/10.1016/0967-0637(95)00013-V.
Jones, E.P., 2001. Circulation in the Arctic Ocean. Polar Res. 20, 139–146. http://dx.doi.org/10.1111/j.1751-8369.2001.tb00049.x.
Jones, E.P., Swift, J.H., Anderson, L.G., Lipizer, M., Civitarese, G., Falkner, K.K., Kattner, G., McLaughlin, F., 2003. Tracing Pacific water in the North Atlantic Ocean. J. Geophys. Res.: Oceans 108, 3116. http://dx.doi.org/10.1029/2001JC001141.
Jones, E.P., Anderson, L.G., Jutterström, S., Mintrop, L., Swift, J.H., 2008. Pacific freshwater, river water and sea ice meltwater across Arctic Ocean basins: results from the 2005 Beringia Expedition. J. Geophys. Res.: Oceans 113, C08012. http://dx.doi.org/10.1029/2007JC004124.
Karl, D.M., Tillbrook, B.D., 1994. Production and transport of methane in oceanic particulate organic matter. Nature 368, 732–734. http://dx.doi.org/10.1038/368732a0.
Karl, D.M., Beversdorf, L., Björkman, K., Church, M.J., Martinez, A., DeLong, E.F., 2008. Aerobic production of methane in the sea. Nat.: Geosci. 1, 473–478. http://dx.doi.org/10.1038/ngeo234.
Kiene, R.P., Slezak, D., 2006. Low dissolved DMSP concentrations in seawater revealed by small volume gravity filtration and dialysis sampling. Limnol. Oceanogr.: Methods 4, 80–95. http://dx.doi.org/10.4319/lom.2006.4.80.
Kirst, G., Thiel, C., Wolff, H., Nothnagel, J., Wanzek, M., Ulmke, R., 1991. Dimethylsulfoniopropionate (DMSP) in ice algae and its possible biological role. Mar. Chem. 35, 381–388. http://dx.doi.org/10.1016/S0304-4203(09)90030-5.
Kitidis, V., Upstill-Goddard, R.C., Anderson, L.G., 2010. Methane and nitrous oxide in surface water along the North-West Passage, Arctic Ocean. Mar. Chem. 121, 80–86. http://dx.doi.org/10.1016/j.marchem.2010.03.006.
Klawonn, I., Bonaglia, S., Brüchert, V., Ploug, H., 2015. Aerobic and anaerobic nitrogen transformation processes in N_2-fixing cyanobacterial aggregates. Int. Soc. Microb. Ecol. 9, 1456–1466. http://dx.doi.org/10.1038/ismej.2014.232.
Knittel, M., Boetius, A., 2009. Anaerobic oxidation of methane: progress with an unknown process. Annu. Rev. Microbiol. 63, 311–334. http://dx.doi.org/10.1146/annurev.micro.61.080706.093130.
Lamontagne, R.A., Swinnerton, J.W., Linnenbom, V.J., Smith, W.D., 1973. Methane concentrations in various marine environments. J. Geophys. Res.: Oceans Atmospheres 78, 5317–5324. http://dx.doi.org/10.1029/JC078i024p05317.
Latysheva, N., Junker, V.L., Palmer, W.J., Codd, G.A., Barker, D., 2012. The evolution of nitrogen fixation in cyanobacteria. Bioinformatics 28, 603–606. http://dx.doi.org/10.1093/bioinformatics/bts008.
Levasseur, M., Gosselin, M., Michaud, S., 1994. A new source of dimethylsulfide (DMS) for the Arctic atmosphere: ice diatoms. Mar. Biol. 121, 181–187. http://dx.doi.org/10.1007/BF00346748.
Longhurst, A., 1998. Ecological Geography of the Sea. Academic Press, New York, 398.
Loose, B., McGillis, W.R., Schlosser, P., Perovich, D., Takahashi, T., 2009. Effects of freezing, growth, and ice cover on gas transport processes in laboratory seawater experiments. Geophys. Res. Lett. 36, L05603. http://dx.doi.org/10.1029/2008GL036318.
Marty, D., Bonin, P., Michotey, V., Bianchi, M., 2001. Bacterial biogas production in coastal systems affected by freshwater inputs. Cont. Shelf Res. 21, 2105–2115. http://dx.doi.org/10.1016/S0278-4343(01)00045-0.
Moisander, P.H., Serros, T., Paerl, R.W., Beinart, R.A., Zehr, J.P., 2014. Gammaproteobacterial diazotrophs and nifH gene expression in surface waters of the South Pacific Ocean. Int. Soc. Microb. Ecol. 8, 1962–1973. http://dx.doi.org/10.1038/ismej.2014.49.
Morata, N., Seuthe, L., 2014. Importance of bacteria and protozooplankton for faecal pellet degradation. Oceanologia 56, 565–581. http://dx.doi.org/10.5697/oc.55-3.565.
Mundy, C.J., Barber, D.G., Michel, C., 2005. Variability of snow and ice thermal, physical and optical properties pertinent to sea ice algae biomass during spring. J. Mar. Syst. 58, 107–120. http://dx.doi.org/10.1016/j.jmarsys.2005.07.003.
Murrell, J.C., 2010. The aerobic methane oxidizing bacteria (Methanotrophs). In: Timmis, Kenneth N. (Ed.), Handbook of Hydrocarbon and Lipid Microbiology, 1953–1966. http://dx.doi.org/10.1007/978-3-540-77587-4_143.
Perovich, D., Meier, W., Tschudi, M., Gerland, S., Richter-Menge, J., 2012. Sea Ice [in Arctic Report Card 2012]. http://www.arctic.noaa.gov/reportcard.
Punshon, S., Azetsu-Scott, K., Lee, A.M., 2014. On the distribution of dissolved methane in Davis Strait, North Atlantic Ocean. Mar. Chem. 161, 20–25. http://dx.doi.org/10.1016/j.marchem.2014.02.004.
Randall, K., Scarratt, M., Levasseur, M., Michaud, S., Xie, H., Gosselin, M., 2012. First measurements of nitrous oxide in Arctic sea ice. J. Geophys. Res.: Oceans 117, C00G15. http://dx.doi.org/10.1029/2011JC007340.
Reeburgh, W.S., 2007. Oceanic methane biogeochemistry. Chem. Rev. 107, 486–513. http://dx.doi.org/10.1021/cr050362v.
Rudels, B., Larsson, A.M. and Sehlstedt, P.I., 1991. . Stratification and water mass formation in the Arctic Ocean: some implications for the nutrient distribution, in: Proceedings of the pro Mare Symposium on Polar Marine Ecology, Trondheim. Sakshaug. E., Hopkins, C.C.E., Øritsland, N.A. (Eds). Polar Research, 10, pp. 19–31.
Rudels, B., Anderson, L.G., Jones, E.P., 1996. Formation and evolution of the surface mixed layer and halocline of the Arctic Ocean. J. Geophys. Res.: Oceans 101, 8807–8821. http://dx.doi.org/10.1029/96JC00143.
Rudels, B., Schauer, U., Björk, G., Korhonen, M., Pisarev, S., Rabe, B., Wisotzki, A., 2013. Observations of water masses and circulation with focus on the Eurasian Basin of the Arctic Ocean from the 1990s to the late 2000s. Ocean Sci. 9, 147–169. http://dx.doi.org/10.5194/os-9-147-2013.
Schäfer, H., 2007. Isolation of Methylophaga spp. from marine dimethylsulfide-degrading enrichment cultures and identification of polypeptides induced during growth on dimethylsulfide. Appl. Environ. Microbiol. 73, 2580–2591. http://dx.doi.org/10.1128/AEM.02074-06.
Schlosser, P., Kromer, B., Ekwurzel, B., Bönisch, G., McNichol, A., Schneider, R., von Reden, R.K., Östlund, H.G., Swift, J.H., 1997. The first trans-arctic ^{14}C section: comparison of the mean ages of the deep waters in the Eurasian and Canadian basins of the Arctic Ocean. Nucl. Inst. Methods Phys. Res. B 123, 431–437. http://dx.doi.org/10.1016/s0168-583x(96)00677-5.
Scott, B.E., Sharples, J., Ross, O.N., Wang, J., Pierce, G.J., Camphuysen, C.J., 2010. Sub-surface hotspots in shallow seas: finescale limited locations of top predator foraging habitat indicated by tidal mixing and sub-surface chlorophyll. Mar. Ecol. Prog. Ser. 408, 207–226. http://dx.doi.org/10.3354/meps08552.
Scranton, M.I., Brewer, P.G., 1978. Consumption of dissolved methane in the deep ocean. Limnol. Oceanogr. 23, 1207–1213. http://dx.doi.org/10.4319/lo.1978.23.6.1207.
Serreze, M.C., Holland, M.M., Stroeve, J., 2007. Perspective on the Arctic's shrinking sea-ice cover. Science 315, 1533–1536. http://dx.doi.org/10.1126/science.1139426.
Serreze, M.C., Stroeve, J., 2015. Arctic sea ice trends, variability and implications for seasonal ice forecasting. Philos. Trans. R. Soc. A: Math., Phys. Eng. Sci. 373, 2045. http://dx.doi.org/10.1098/rsta.2014.0159.
Shakhova, N., Semiletov, I., Salyuk, A., Yusupov, V., Kosmach, D., Gustafsson, O., 2010. Extensive methane venting to the atmosphere from sediments of the East Siberian Arctic Shelf. . Sci. 327, 1246–1250. http://dx.doi.org/10.1126/science.1182221.
Shiozaki, T., Ijichi, M., Isobe, K., Hashihama, F., Nakamura, K.-i., Ehama, M., Hayashizaki, K.-i., Takahashi, K., Hamasaki, K., Furuya, K., 2016. Nitrification and its influence on biogeochemical cycles from the equatorial Pacific to the Arctic Ocean. Int. Soc. Microb. Ecol. 1–14, 1751–7370. http://dx.doi.org/10.1038/ismej.2016.18.
Smith, A.J., Mienert, J., Bünz, S., Greinert, J., 2014. Thermogenic methane injection via bubble transport into the upper Arctic Ocean from the hydrate-charged Vestnesa Ridge, Svalbard. Geochem. Geophys. Geosyst. 15, 1945–1959. http://dx.doi.org/10.1002/2013GC005179.
Spreen, G., Kaleschke, L., Heygster, G., 2008. Sea ice remote sensing using AMSR-E 89 GHz channels. J. Geophys. Res. 113, C02S03. http://dx.doi.org/10.1029/2005JC003384.
Steinle, L., Graves, C.A., Treude, T., Ferré, B., Biastoch, A., Bussmann, I., Berndt, C., Krastel, S., James, R.H., Behrens, E., Böning, C.W., Greinert, J., Sapart, C.J., Scheinert, M., Sommer, S., Lehmann, M.F., Niemann, H., 2015. Water column methanotrophy controlled by a rapid oceanographic switch. Nat. Geosci.: Lett. 8, 378–382. http://dx.doi.org/10.1038/ngeo2420.
Sun, J., Steindler, L., Thrash, J.C., Halsey, K.H., Smith, D.P., Carter, A.E., Landry, Z.C., Giovannoni, S.J., 2011. One Carbon Metabolism in SAR11 Pelagic Marine Bacteria. PLoS ONE, 6. http://dx.doi.org/10.1371/s0023973.
Swift, J.H., Takahashi, T., Livingston, H.D., 1983. The contribution of the Greenland and Barents seas to the deep water of the Arctic Ocean. J. Geophys. Res.: Oceans 88, 5981–5986. http://dx.doi.org/10.1029/JC088iC10p05981.
Tolar, B.B., Ross, M.J., Wallsgrove, N.J., Liu, Q., Aluwihare, L.I., Popp, B.N., Hollibaugh, J.T., 2016. Contribution of ammonia oxidation to chemoautotrophy in Antarctic coastal waters. Int. Soc. Microb. Ecol., 1–15. http://dx.doi.org/10.1038/ismej.2016.61.
Tovar-Sánchez, A., Duarte, C.M., Alonso, J.C., Lacorte, S., Tauler, R., Galbán-Malagón, C., 2010. Impacts of metals and nutrients released from melting multiyear Arctic sea ice. J. Geophys. Res.: Oceans 115, C07003. http://dx.doi.org/10.1029/2009JC005685.
Wallmann, K., Pinero, E., Burwicz, E., Haeckel, M., Hensen, M., Dale, A., Ruepke, L., 2012. The global inventory of methane hydrate in marine sediments: a theoretical approach. Energies 5, 2449–2498. http://dx.doi.org/10.3390/en5072449.
Westbrook, G.K., Thatcher, K.E., Rohling, E.J., Piotrowski, A.M., Pälike, H., Osborne, A.H., Nisbet, E.G., Minshull, T.A., Lanoisellé, M., James, R.H., Hühnerbach, V., Green, D., Fisher, R.E., Crocker, A.J., Chabert, A., Bolton, C., Beszczynska-Möller, A., Berndt, C., Aquilina, A., 2009. Escape of methane gas from the seabed along the West Spitsbergen continental margin. Geophys. Res. Lett. 36, L15608. http://dx.doi.org/10.1029/2009GL039191.
Wrage, N., Velthof, G.L., van Beusichem, M.L., Oenema, O., 2001. Role of nitrifier denitrification in the production of nitrous oxide. Soil Biol. Biogeochem. 33, 1723–1732. http://dx.doi.org/10.1016/S0038-0717(01)00096-7.
Yamamoto-Kawai, M., Carmack, E., McLaughlin, F., 2006. Nitrogen balance and Arctic throughflow. Nat. Brief Commun. 443, 43. http://dx.doi.org/10.1038/443043a.